Extremophiles (2008) 12:325–333
DOI 10.1007/s00792-007-0131-9

ORIGINAL PAPER

Purine nucleoside phosphorylase from *Pseudoalteromonas* sp. Bsi590: molecular cloning, gene expression and characterization of the recombinant protein

Xiaohui Li · Xinyin Jiang · Huirong Li · Daming Ren

Received: 25 July 2007 / Accepted: 22 November 2007 / Published online: 26 February 2008

Abstract The gene encoding purine nucleoside phosphorylase (PNP) from the cold-adapted marine bacterium *Pseudoalteromonas* sp. Bsi590 was identified, cloned and expressed in *Escherichia coli*. The gene encodes a polypeptide of 233 amino acids with a calculated molecular weight of 25,018 Da. *Pseudoalteromonas* sp. Bsi590 PNP (*Pi*PNP) shares 60% amino sequence identity and conservation of amino acid residues involved in catalysis with mesophilic *Escherichia coli deoD*-encoded purine nucleoside phosphorylase (*Ec*PNP). N-terminal his-tagged *Pi*PNP and *Ec*PNP were purified to apparent homogeneity using Ni^{2+}-chelating column. Compared with *Ec*PNP, *Pi*PNP possessed a lower temperature optimum and thermal stability. As for PNP enzymes in general, *Pi*PNP and *Ec*PNP displayed complicated kinetic properties; *Pi*PNP possessed higher K_m and catalytic efficiency (k_{cat}/K_m) compared to *Ec*PNP at 37°C. Substrate specificity results showed *Pi*PNP catalyzed the phosphorolytic cleavage of 6-oxopurine and 6-aminopurine nucleosides (or 2-deoxynucleosides), and to a lesser extent purine arabinosides. *Pi*PNP showed a better activity with inosine while no activity toward pyrimidine nucleosides. The protein conformation was analyzed by temperature perturbation difference spectrum. Results showed that *Pi*PNP had lower conformation transition point temperature than *Ec*PNP; phosphate buffer and KCl had significant influence on *Pi*PNP protein conformation stability and thermostability.

Keywords *Pseudoalteromonas* · *Escherichia coli* · Purine nucleoside phosphorylase · Characterization

Abbreviations

*Pi*PNP	*Pseudoalteromonas* sp. Bsi590 purine nucleoside phosphorylase
*Ec*PNP	*Escherichia coli* purine nucleoside phosphorylase

Introduction

The ubiquitous purine nucleoside phosphorylase [(PNP, purine nucleoside: ortho-phosphate ribosyl transferase (EC 2.4.2.1.)], a key enzyme of purine metabolism in the salvage pathway, catalyzes the reversible phosphorolysis of (2′-deoxy) purine nucleosides to the free purine base and (2′-deoxy) ribose-1-phosphate. PNPs from different organisms have been identified so far. The properties and functions of the enzymes were reviewed by Bzowska et al. (2000). Mammalian PNPs, such as those from human erythrocytes and bovine spleen, are trimeric and have a monomeric molecular weight of 31 kDa (Parks and Agarwal 1972; Stoeckler et al. 1978), whereas most prokaryotic PNPs are hexameric with a monomeric molecular weight of 26 kDa (Jensen and Nygaard 1975; Ling et al. 1994). In general, PNPs with a trimeric structure accept only guanosine and inosine as substrates, whereas the hexameric PNPs accept adenosine as well as

Communicated by K. Horikoshi.

X. Li · X. Jiang · D. Ren (✉)
The State Key Laboratory of Genetic Engineering,
Institute of Genetics, Fudan University,
200433 Shanghai, China
e-mail: dmren@fudan.edu.cn

H. Li
SOA Key Laboratory for Polar Science,
Polar Research Institute of China,
200136 Shanghai, China

guanosine and inosine. Based on the substrate difference between *Escherichia coli* and human, this enzyme is being evaluated as a suicide gene therapy strategy for the treatment of solid tumors (Sorscher et al.1994; Hughes et al. 1995; Yang et al. 2005). Certain prodrugs, such as 6-methylpurine-2′-deoxyriboside, are not cleaved by human PNP when they are injected into tumor cells transfected with the *E. coli* PNP gene; however, the nontoxic 6-methylpurine-2'-deoxyriboside is converted by bacterial PNP to the highly cytotoxic base, 6-methylpurine, and an excellent in vivo bystander activity has also been demonstrated by these agents. PNP is also involved in the enzymatic synthesis of nucleosides, where the enzyme operates in the reverse direction (Krenitzky and Koszalka 1981; Utagawa et al. 1985; Elizabeth et al. 2000).

There are many reports on psychrophilic enzymes from low temperature microbiology (Feller et al. 1996; Lorentzen et al. 2006). The cold-adapted microorganism is an excellent candidate for investigations of protein evolution and molecular adaptations to extreme conditions. Cold active enzyme shows a high specific activity at low temperatures, a low temperature optimum and a limit thermal stability, resulting in a rapid inactivation at moderate temperature. It is assumed that cold active enzyme is more flexible than their mesophilic counterparts (for a review, see Feller and Gerday 1997). The available data suggest that the mesophilic *E. coli deoD*-encoded PNP (*Ec*PNP) and the hyperthermophilic archaeal 5'-deoxy-5'-methylthioadenosine phosphorylase from *S. solfataricus* (ssMTAP) possess the greatest temperature diversity, although both share a similar structural organization from the established crystal structures (Appleby et al. 2001; Pugmire and Ealick 2002). Physicochemical characteristics and structure knowledge of PNP from the low temperature organisms has not been reported yet. Under this concern, we searched the genome databases of psychrophilic bacteria and found an open reading frame designated inosine phosphorylase (PNP, PSHAb0082) by genome project in the cold-adapted *Pseudoalteromonas haloplanktis* TAC125 (Claudine et al. 2005), but experimental data of its catalytic activity were unidentified. It is of interest that the PNP proteins of *Pseudoalteromonas haloplanktis* TAC125 were found to be evolutionarily conserved with those of mesophilic and thermophilic bacteria; further identification of the biophysical properties of psychrophilic PNP enzymes can increase the knowledge about structural patterns underlying cold adaptation. In this study, according to the homologous gene sequence, we have successfully cloned the PNP from *Pseudoalteromonas* sp. Bsi590 (*Pi*PNP) and several characteristics of the His-tagged recombination enzymes were examined, compared with mesophilic *Ec*PNP.

Materials and methods

Materials

Xanthine oxidase and inosine were purchased from Sigma (USA); pMD18-T vector, restriction enzymes and DNA ligase were purchased from Takara (Dalian, China); isopropyl-thio-β-D-galactoside (IPTG) was purchased from Shenggong Corporation (Shanghai, China); oligonucleotides synthesis and DNA sequencing were performed in Shenggong Corporation (Shanghai, China).

6-Methylpurine-2′-deoxyriboside was prepared from 6-methylpurine and 2′-deoxyuridine by the method of Gao et al. (2007) with a purity of 99.3% by HPLC. All chemicals employed were of the highest quality commercially available. *Pseudoalteromonas* sp. Bsi590 isolated from the Arctic sea ice was kindly provided by Dr. Huirong Li (Polar Research Institute of China, Shanghai).

The plasmid pET-DH harboring *E. coli deoD*-encoded PNP was constructed with the expression vector pET28b using *Eco*R I and *Sal* I digestion reported previously (Li et al. 2006) and transformed into *Escherichia coli* Rosetta (DE3) pLysS for enzyme preparation.

Gene cloning

PNP gene from *Pseudoalteromonas* sp. Bsi590 was amplified by PCR, using a set of oligonucleotide primers; the primers contained *Eco*R I and *Sal* I sites (underlined), respectively, as follows: CCGGAATTCGATG(G/A/T)(G/C)(G/T)ACTCCGCATAT(C/T)(A/G)ATGC (forward) and GCGTCGACTTAGATAGACTC (reverse). The PCR product was inserted by T4 DNA ligase into pMD18-T cloning vector, transformed in *E. coli* DH5α cells and sequenced. The resultant plasmid was digested with *Eco*R I and *Sal* I, and subcloned into the corresponding sites of pET28b to yield the expression plasmid pETi590. The nucleotide sequence data have been deposited in the NCBI database under the accession number EF222283.

Protein expression and purification of the PNP in *E. coli*

Plasmid pETi590 was introduced into *Escherichia coli* Rosetta (DE3) pLysS via transformation. A single colony was grown overnight at 37°C in LB medium containing 50 μg/ml kanamycin and 34 μg/ml chloramphenicol. The saturated culture was then diluted 1:100 in 100 ml LB medium supplemented with kanamycin and chloramphenicol and grown with shaking at 37°C. When the cells reached $A_{600\ nm}$ of 0.8, protein expression was induced by the addition of 1 mM IPTG. After a further 8 h of growth,

the cells were harvested by centrifugation at 4°C and washed with 20 mM Tris–HCl (pH 7.5). Cells were disrupted by sonication on ice (300 W, 30 min) followed by a removal of the debris by centrifugation (10,000 rpm, 30 min, 4°C). His-tagged recombinant PNP was purified with Ni^{2+} affinity chromatography column using the QIA expression kit (Qiagen) by following native protein purification protocol, with the following two modifications: phosphate buffer was replaced by Tris–HCl and elution was done using 250 mM imidazole. Fractions were then concentrated to about 1/10th of the volume using an Amicon Ultra-15 spin column (Millipore). Purified PNP was identified by SDS-PAGE.

Expression of *Ec*PNP was performed in 100 ml batch fermentation at 37°C as described above, and about 14 mg of recombinant protein with a calculated molecular weight of 29.7 kDa was purified to homogeneity as determined by SDS-PAGE.

Protein analytical assays

Purity of the preparation was checked by SDS-PAGE in 12% gels, followed by staining with Coomassie brilliant blue R250, according to standard procedures (Sambrook and Russell 2002). The protein concentration was determined by the method of Bradford, using bovine serum albumin as standard.

Enzyme activity measurements

PNP activity was measured in the phosphorolysis direction from inosine to hypoxanthine. The standard incubation mixture contained 0.5 mM inosine and 25 mM sodium phosphate buffer (pH 7.5) in a final volume of 200 µl. The reaction was done at 37°C for 10 min; the produced hypoxanthine was transformed into uric acid using a coupled reaction with xanthine oxidase (0.05 U/reaction) (Bennett et al. 2003). The latter reaction was done at 25°C for 1 h. Appearance of uric acid in the reaction was then monitored by its specific absorbance at 293 nm ($\varepsilon = 133\ \mu M^{-1}\ cm^{-1}$). Specific activity was expressed as micromoles of produced hypoxanthine per minute per milligram of protein at 37°C.

pH and temperature optimum measurements

The pH-optimum of the *Pi*PNP was determined using the following 50 mM buffers: citric acid with pH range 3.0–5.0, sodium phosphate with pH range 6.0–8.0, and glycine–NaOH with pH range 8–11. The temperature dependence of the activity of *Pi*PNP and *Ec*PNP was determined in 25 mM sodium phosphate buffer (pH 7.5) at temperatures from 0 to 70°C, using inosine as a substrate. Residual activity was calculated setting highest activity measured to 100%.

pH and temperature stability measurements

*Pi*PNP was mixed with different pH buffer on ice for 2.5 h and the activity was determined using inosine as a substrate. Thermostability of the enzyme was measured in 20 mM Tris–HCl (pH 7.5) at 0, 18, 37, 42, 50, 55, 60, and 65°C by incubating the enzyme in thin-wall microtubes for 30 min, followed by chilling the tubes in an ice-water bath. A portion of the sample was used to determine the activity using inosine as a substrate. Residual activity was calculated setting highest activity measured to 100%.

Determination of K_m and k_{cat}

The kinetic parameters of *Pi*PNP- and *Ec*PNP-catalyzed reaction were determined at a 600 µl volume containing 50 mM sodium phosphate buffer (pH7.5) with inosine concentrations ranging from 25 µM to 0.7 mM at 18, 37, and 55°C, and the protein contents were 120 and 80 ng for *Pi*PNP and *Ec*PNP, respectively. When the kinetic parameters for phosphate were assayed, the phosphate concentration varied from 0.1 to 5 mM and the inosine was kept at 0.5 mM. The Michaelis–Menten parameters were determined from linear double reciprocal plots of 1/velocity versus 1/concentration of the substrate. The best line was determined by linear regression of at least five datum points (the regression coefficient for each measurement was greater than 0.95). Values of K_m and V_{max} were determined from the intercept of the *x*-axis and *y*-axis, respectively. V_{max} values were calculated based on micromoles of hypoxanthine formed per minute per milligram of enzyme protein. Turnover number k_{cat} values were corrected for subunit molecular content for *Pi*PNP and *Ec*PNP.

Substrate specificity

The purified *Pi*PNP was assayed for its ability to metabolize the various purine and pyrimidine nucleosides; the reaction was performed at 37°C for 1 h in 600 µl volume and stopped by boiling the samples for 5 min. The disappearance of the substrates and the appearance of the products were monitored by reverse phase high-pressure

liquid chromatography (HP1100, Agilent Technologies, USA). The amount of purine base formed was determined by measuring the percentage of the absorbance integrated peak area of purine base formed with respect to the total (nucleoside + purine base) absorbance integrated peak areas. Enzyme activity was calculated according to the percentage of purine base formed .The mobile phase was 7% acetonitrile in 50 mM ammonium dihydrogen phosphate at a rate of 1 ml/min.

UV–visible absorption spectrum

The UV–visible absorption spectrum of *Pi*PNP and *Ec*PNP was recorded in 5 mM Tris–HCl (pH 7.5), using V-550 UV/VIS spectrophotometer (Jasco, Tokyo, Japan). Heat-induced unfolding of protein was analyzed by UV spectroscopy. The absorption value at 277 nm was recorded.

Considering the fact that kinetically driven protein unfolding is scan rate- and concentration-dependent, accordingly both *Pi*PNP and *Ec*PNP were recorded at a similar UV-absorption value at the same condition.

Circular dichroism

Circular dichroism (CD) measurements were carried out on Jasco J-715 spectropolarimeter. The protein samples used for CD measurements were about 12 μg/ml. The CD spectra were analyzed in the 200–250 nm region in a 0.05 cm quartz cell at room temperature.

Results

Gene cloning and sequence analysis

PNP sequence in genome of *Pseudoalteromonas haloplanktis* TAC125 was sought; the ORF contains 702 bp coding for a polypeptide of 233 amino acids. Multiple alignments were performed using CLUSTAL W (Thompson et al. 1997). *P. haloplanktis* PNP showed high identity with PNP-related proteins: 59.8% with PNP from *E. coli*, 58.8% with PNP from *E. aerogenes*, 57.9% with PNP from *E. carotovora*. Residues involved in the substrate-binding and catalysis sites were highly conserved (Fig. 1). According to the conserved N-terminal sequence of PNP proteins and C-terminal sequence of *Pseudoalteromonas haloplanktis* TAC125, the complete gene sequence was successfully amplified from *Pseudoalteromonas* sp. Bsi590 and deposited in Genbank (accession number EF222283). The deduced amino acid sequence displayed 96 and 60% of identity with *P. haloplanktis* TAC125 PNP and *E. coli*

Fig. 1 Sequence comparison of PNPs from various species: Ec, *E. coli* PNP (NCBI accession no. NP418801); Ea, *E. aerogenes* PNP; Er, *E. carotovora* PNP (Li et al. 2006); Ph, *Pseudoalteromonas haloplanktis* TAC125 PNP (NCBI accession no. YP341578); Pi, *Pseudoalteromonas* sp. Bsi590 PNP (NCBI accession no. EF222283); Ss, *Sulfolobus solfataricus* MTAP (NCBI accession no. NC002754). Residues conserved in proteins are shaded. The positions at the phosphate (*star*), Pentose (*triangle*), and base (*closed circle*) binding sites of *E. coli* PNP are indicated according to Yang et al. (2005). Numbers on the left are the coordinates of each protein

PNP, respectively. The proposed active-site residues in *Ec*PNP, i.e., His4, Gly20, Arg24, Arg43, Arg89, Asp112, Leu158, Phe159, Met180, Glu181, Asp204, are conserved in the *Pseudoalteromona* PNPs sequence. Alignment with other PNP proteins showed significant homology surrounding phosphate binding site and catalysis site, forming the consensus amino sequences GDPLRA and TVSDH, respectively.

Expression and purification of the recombinant enzyme

To prove its coding function, *Pseudoalteromonas* sp. Bsi590 PNP (*Pi*PNP) was overexpressed in *Escherichia*

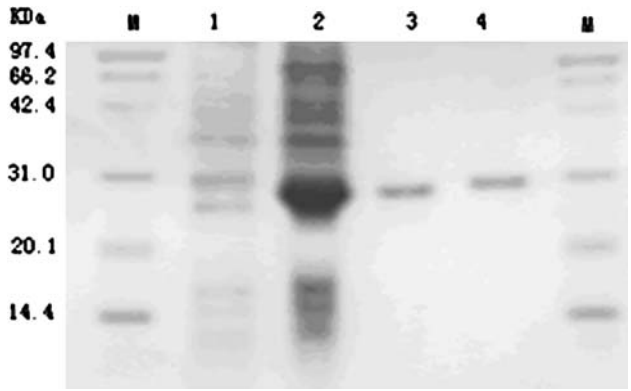

Fig. 2 SDS-PAGE (12% acrylamide) analysis of recombinant PNPs. Protein bands were stained with Coomassie brilliant blue R-250. *Lanes 1* and *2* are the noninduced and induced cell samples from *Pi*PNP expressed in *E. coli* strains Rosseta (DE3) pLys S; *Lanes 3* and *4* are the purified *Pi*PNP and *Ec*PNP fractions after concentration by Amicon ultra 15; *Lane M* are the molecular weight markers

coli at 25, 30, and 37°C with the induction of 1 mM IPTG. Under the experimental conditions, different induction temperatures had no significant influence on the PNP protein folding, as PNPs were mainly in soluble form in the cell lysate after sonication. About 18 mg of *Pi*PNP enzyme preparation was obtained from 100 ml culture with a specific activity of about 204 U/mg. The purity of purified enzyme was found to be more than 90% by Coomassie-staining of SDS-PAGE gels (Fig. 2); the final preparation revealed a single band with a molecular weight of about 29 kDa, which is consistent with the expected mass deduced from the primary amino acid sequence of the recombinant enzyme.

pH and temperature properties of recombinant enzyme

The effect of pH on *Pi*PNP enzymatic activity was investigated in the pH range 4–11; the optimum pH corresponded to the pH-dependent stability profile of reaction, with an optimum between pH 8 and 10 and stable for 2.5 h at pH 10, only about half of the maximal activity at acid condition, respectively (data not shown).

The *Pi*PNP and *Ec*PNP assays were performed in 25 mM sodium phosphate buffer (pH 7.5) with 0.5 mM inosine as substrate; temperatures varied from 0 to 65°C as shown in Fig. 3. A broad optimal temperature for *Pi*PNP was 30–35°C .At 0°C (on ice-water), 35% of the maximal activity was observed, while *Ec*PNP showed optimum temperature of 60°C.

To determine the thermostability, the enzymes were incubated for 30 min in 20 mM pH 7.5 Tris–HCl at a particular temperature before measuring the residual activity under standard conditions. The *Pi*PNP was stable

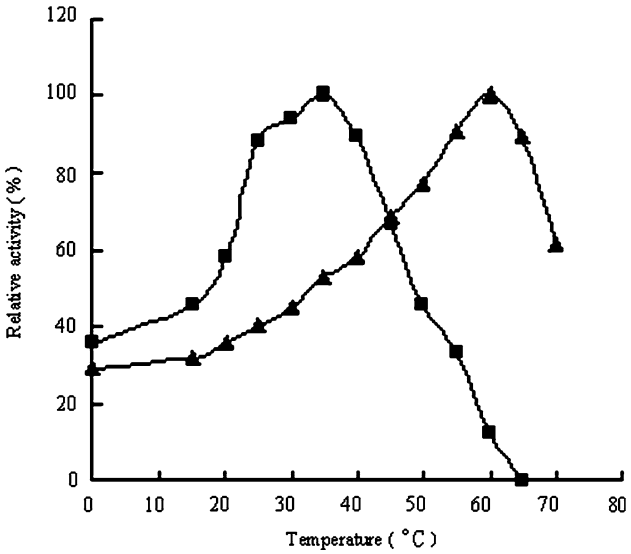

Fig. 3 Temperature optimum profile for recombinant *Ec*PNP (*triangle*) and *Pi*PNP (*square*)

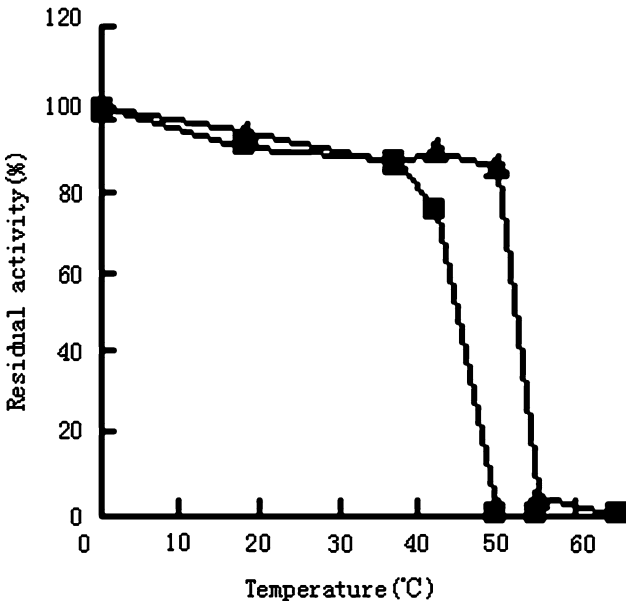

Fig. 4 Thermostability of *Ec*PNP (*triangle*) and *Pi*PNP (*square*). The thermostability was determined by incubating the enzyme at 20 mM Tris–HCl (pH 7.5) at a particular temperature for 30 min and then placing it on ice before measuring the activity under standard assay conditions at 37°C. In both cases, the maximum activity corresponds to a specific activity of 200 U/mg; the highest activity was set to 100%

upto 37°C; a decrease in its activity was observed above 37°C, retaining only 74% of its original activity at 42°C and reaching total inactivation at 50°C (Fig. 4). *Ec*PNP retained 85% of its activity at 50°C, but the activity decreased drastically at 55°C and was totally inactivated at 65°C.

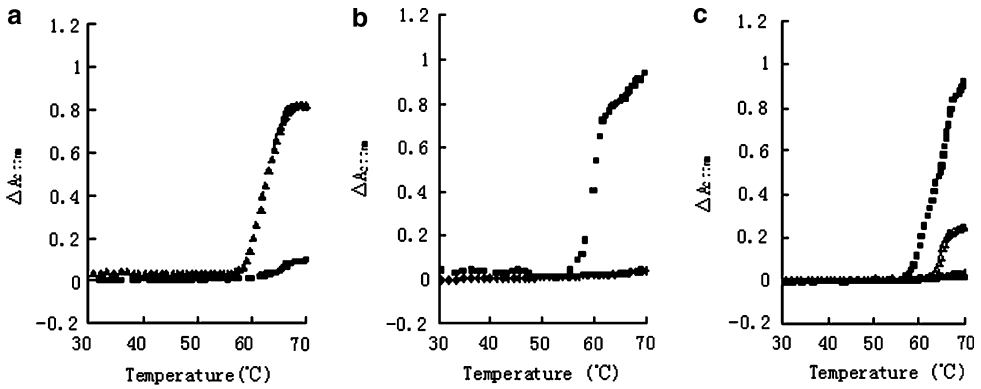

Fig. 5 The temperature perturbation difference spectra of recombinant PNPs. **a** Thermal unfolding of *Ec*PNP (*square*) and *Pi*PNP (*triangle*) in the presence of 5 mM Tris–HCl. **b** Thermal unfolding of *Pi*PNP in the presence of 20 mM Tris–HCl (*square*) and phosphate buffer (*diamond*). **c** Thermal unfolding of *Pi*PNP with the addition of KCl. (*square*) Without KCl, (*unfilled triangle*) 0.5 M KCl, (filled triangle) 1 M KCl

Temperature perturbation difference spectrum analysis

According to the sequence analysis results, *Pi*PNP and *Ec*PNP proteins have Phe and Tyr but no Trp residues. The UV–visible absorption spectrums of both proteins were scanned between 190 and 500 nm, which presented major peaks at 277 nm. These spectroscopic properties are common to other PNPs (Tebbe et al. 1997).

Heat-induced unfolding of *Pi*PNP and *Ec*PNP protein was analyzed by 277 nm UV spectroscopy between 20 and 70°C. *Pi*PNP and *Ec*PNP thermal unfolding processes were irreversible. The beginning point of the transition of the *Pi*PNP was 58°C, which was lower than that of the *Ec*PNP enzyme (62°C) in 5 mM Tris–HCl buffer (Fig. 5a). *Pi*PNP was more stable in 50 mM phosphate buffer than in Tris–HCl buffer, since the UV absorption change was little (Fig. 5b). *Pi*PNP conformation transition was recorded at different KCl concentrations as shown in Fig. 5c. The KCl induced strong enzyme conformation stabilization: 0.5 M KCl markedly increased the conformation transition point temperature from 58 to 63°C; 1 M KCl induced least changes of the UV absorption indicating high ionic strength, and promoted the *Pi*PNP conformation stability.

Direct evidence that KCl and phosphate affected the enzyme stability had been provided by the comparison of the residual activity of *Pi*PNP in the absence and presence of KCl and phosphate. The *Pi*PNP was incubated at a defined temperature from 35 to 50°C. After 1 h of incubation at 50°C with 0.5 M KCl and 1 M KCl, the enzyme activities still retained 81 and 38%, respectively, whereas it was inactivated without KCl (Fig. 6a). As shown in Fig. 6b, phosphate exerts a protection toward temperature inactivation of the enzyme; after 1 h of incubation at 45°C, it retained 84 and 57% of its catalytic activity in the presence of 50 and 100 mM sodium phosphate comparing with 45% activity when the enzyme was incubated alone. The enzyme retained higher residual activity at high concentration of substrates. This result indicated that the binding of this substrate raised the conformational stability of the enzyme, thus reducing its susceptibility to thermal denaturation.

Kinetic properties of *Pi*PNP and *Ec*PNP

The kinetic parameters for inosine and phosphate are reported in Table 1. As expected for PNPs, when the variable substrate was inosine, the reaction kinetics displayed a mixture of negative and positive cooperativity, as well as substrate inhibition at high concentration. But within low inosine concentration ranging from 50 to 600 μM at 37°C for *Pi*PNP, and at 37 and 55°C for *Ec*PNP, the linear Michaelis–Menten kinetics plots were observed. K_m for inosine at 37°C was about two times higher for *Pi*PNP than that for *Ec*PNP; the catalytic efficiency, k_{cat}/K_m, for inosine at 37°C was 1.2-fold higher for *Pi*PNP when compared to that for *Ec*PNP at the same temperature. *Ec*PNP showed higher k_{cat} and K_m values at 55°C; the catalytic efficiency, k_{cat}/K_m, for phosphate was four times higher for *Pi*PNP than that for *Ec*PNP.The velocity of *Pi*PNP increased at 18 and 37°C but decreased at 55°C, whereas from 37 to 55°C, *Ec*PNP increased with increasing temperature, in line with our previous observations on the enzyme optimum activity.

Substrate specificity to nucleosides

Like the homologous hexameric PNP, *Pi*PNP was characterized by a broad substrate specificity that recognized purine nucleosides with substitutions in the 6-position, such as adenosine, inosine, guanosine, and 6-methyl purine nucleosides, serving as substrates (Table 2). When inosine

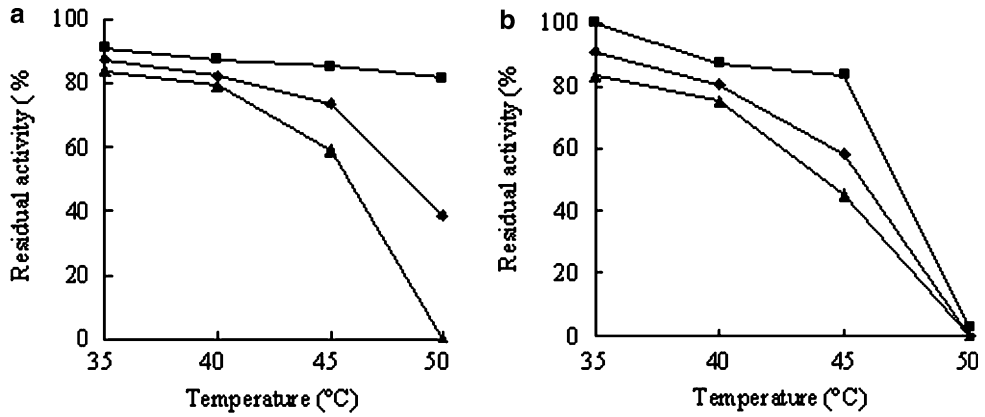

Fig. 6 Effect of different additives on the thermostability of *Pi*PNP. **a** Residual *Pi*PNP activity after 1 h of incubation at temperatures shown in the absence (*triangle*) or in the presence of 0.5 M KCl (*diamond*) and 1 M KCl (*square*), respectively. **b** Residual *Pi*PNP activity after 1 h of incubation at temperatures shown in the absence (*triangle*) or in the presence of 50 mM phosphate (*diamond*) and 100 mM phosphate (*square*), respectively. Samples containing 0.3 mg/ml were incubated in 20 mM Tris–HCl (pH 7.5) or in the presence of KCl and phosphate, respectively. Aliquots (1 µl) were then withdrawn and assayed for PNP activity as described in "Material and methods." Activity values are expressed as percentage of the time-zero control (100%)

Table 1 Kinetic apparent parameters for *Pi*PNP and *Ec*PNP

Enzyme	Assay temperature (°C)	Apparent K_m (mM) for		V_{max} (U/mg)	k_{cat} (S^{-1})	k_{cat}/K_m (M^{-1} S^{-1}) for	
		Inosine	Phosphate			Inosine	Phosphate
*Pi*PNP	37	0.67	0.21	235.85	113.60	1.7×10^5	5.65×10^4
*Ec*PNP	37	0.32	0.34	90.47	44.93	1.4×10^5	1.42×10^4
	55	0.83	–	211.27	104.94	1.26×10^5	–

Table 2 Substrate specificity of *Pi*PNP

Substrate	Relative activity (%)
Purine nucleoside	
Adenosine	15.4 ± 0.6
2′-Deoxyadenosine	13.4 ± 0.3
Inosine	100
Guanosine	55.8 ± 3.6
2′-Deoxyguanosine	3.7 ± 0.6
2′-Deoxy-6-methylpurine	13.2 ± 0.5
Pyrimidine nucleosides	
Uridine	–
2′-Deoxyuridine	–
Cytidine	–
2′-Deoxycytidine	–
2′-Deoxythymidine	–
Arabinose sugars nucleosides	
Arabinofuranosyladenine (Ara-A)	4.3 ± 0.7
Arabinofuranosyluridine (Ara-U)	–

The phosphate concentration was 50 mM in all the assays; the Ara-A concentration was 0.375 mM; others were 0.5 mM in the reaction. Relative activities are expressed relative to inosine (100%). Data are the average value of two repeated experiments

was used as the preferred substrate for *Pi*PNP, the rate of phosphorolysis of ribonucleosides was more efficient than that of deoxyribonucleosides. *Pi*PNP was unable to metabolize the pyrimidine nucleosides and at very low rate arabinofuranosyladenine.

Discussion

Although PNPs are widespread in many organisms, PNP-homologous enzyme characterizations in psychrophilic organism have not been reported yet. By comparing sequences of PNP proteins binding phosphate and nucleoside, we used a pair of degenerate primers to obtain 560 bp N-terminal sequence fragment of PNP gene from eight different *Pseudoalteromonas* spp., which showed 98% similarity to PNP from *Pseudoalteromonas haloplanktis* TAC125 (*Ph*PNP) (unpublished data). Using the conserved N-terminal sequence and C-terminal sequence of *Ph*PNP gene, a full length of 702 bp gene was PCR-amplified from *Pseudoalteromonas* spBsi590. Analysis of the *Pi*PNP amino acid sequence shows 60% identity with *Ec*PNP; the rare condons AGG, CTA, and ATA were used

several times in the sequence; so the *E. coli* Rosetta was used to express *Pi*PNP.

To determine possible cold-adapted features of *Pi*PNP, PNP from *E. coli* was chosen as a mesophilic counterpart due to the high sequence homology; *Pi*PNP optimal temperature was found to be lower than that of mesophilic *Ec*PNP. At low temperature, the catalytic activity was higher for *Pi*PNP than that for *Ec*PNP.

Thermal unfolding results showed protein conformation changed at high temperature, substrate phosphate and KCl can stabilize PNP structure. Being a psychrophilic enzyme, *Pi*PNP was endowed with a significant thermal stability in the presence of phosphate and KCl; this substrate stabilization seems to be a property common to other PNPs belonging to the NP-I family, such as the mesophilic *E. coli* PNP (Koszalka et al. 1988) and the hyperthermophilic SsMTAP (Cacciapuoti et al. 2001). The appreciable stabilization of *Pi*PNP and *Ec*PNP by phosphate and nucleosides, but not by free base hypoxanthine, is consistent with the mechanism proposed for PNP, where all substrates except free bases form binary complexes with the free enzyme.

Kinetic experiments showed that inosine inhibited enzyme activity at high concentration and a non-Michaelis kinetics was observed (Ropp and Traut 1991). Similar nonlinear plots have been observed for PNP from chicken liver (Murakami and Tsushima 1975) and human erythrocytes (Kim et al. 1968) with inosine as the variable substrate. Unfortunately, we cannot accurately determine the K_m value and compare kinetic data between *EcPNP* and *PiPNP*, but the significant structural homology and similar physicochemical properties support the hypothesis that all PNPs shared a common ancestor (Yang et al. 2005). The high sequence similarity with mesophilic PNP may indicate that the ancestor of a psychrophilic enzyme was adapted to higher temperatures.

*Pi*PNP has evolved to maintain a high efficiency at low temperature; eleven residues forming the catalytic and binding sites are strictly conserved in their mesophilic counterparts from *Ec*PNP. This implies that the protein structures outside the active site are responsible for cold-adapted activity. Temperature perturbation difference spectrum results showed that *Pi*PNP had lower conformation transition point than *Ec*PNP, while the analysis of CD spectral properties reveals identical secondary structural content between *Pi*PNP and *Ec*PNP; they both shared 74% helical and 26% β-turn content. Further studies on three-dimensional structure of should give more precise information for the structure–function relationship of this novel enzyme.

*Pi*PNP can accept 6-methyl purine nucleoside as substrates, considering the higher catalytic activity of *Pi*PNP at 37°C than *Ec*PNP at the same temperature; this result may provide attractive candidate for pro-drug activation and nucleoside biotransformation at low temperature. Until now, enzymatic synthesis of nucleoside analogs is still performed at high temperatures of 55–65°C; a reduction in energy consumption is of potential advantage to the biotechnology industry.

Acknowledgments We sincerely thank Dr. Li Huirong of the Polar Reasearch Institute of China for the donation of *Pseudoalteromonas* spp. We are also grateful to the State Key Lab of Genetic Engineering for HPLC and CD measurements. We thank Ji Chaoneng and Hu Hairong for expert technical assistance. This work was financially supported by National Natural Science Foundation of China under the grant number 40376001.

References

Appleby TC, Mathews II, Porcelli M, Cacciapuoti G , Ealick SE (2001) Three-dimensional structure of a hyperthermophilic 5′-deoxy-5′-methylthioadenosine phosphorylase from *Sulfolobus solfataricus*. J Biol Chem 42:39232–39242

Bennett EM, Li CL, Allan PW, Parker WB, Ealick SE (2003) structural basis for substrate specificity of *Escherichia coli* purine nucleoside phosphorylase. J Biol Chem 278:47110–47118

Bzowska A, Kulikowska E, Shugar D (2000) Purine nucleoside phosphorylases: properties, functions, and clinical aspects. Pharmacol Ther 88:349–425

Cacciapuoti G, Servillo L, Moretti M, Porcelli M (2001) Conformational changes and stabilization induced by phosphate binding to 5′-methylthioadenosine phosphorylase from the thermophilic archaeon *Sulfolobus solfataricus*. Extremophiles 5:295–302

Claudine M, Krin E, Pascal G, Barbe V, Bernsel A, Bertin PN, Cheung F, Cruveiller S, D'Amico S, Duilio A, Fang G, Feller G, Ho C, Mangenot S, Marino G, Nilsson J, Parrilli E, Rocha EPC, Rouy Z, Sekowska A, Tutino ML, Vallenet D, Heijne GV, Danchin A (2005) Coping with cold: the genome of the versatile marine Antarctica bacterium *Pseudoalteromonas haloplanktis* TAC125. Genome Res 15:1325–1335

Elizabeth SL, Martinez N, Rogert MC (2000) An improved microbial synthesis of purine nucleosides. Biotechnol Lett 22:1277–1280

Feller G, Gerday C (1997) Psychrophilic enzymes: molecular basis of cold adaptation Cell. Mol Life Sci 53:830–841

Feller G, Narinx E, Arpigny JL, Aittaleb M, Baise E, Genicot S (1996) Enzymes from psychrophilic organisms. FEMS Microbiol Rev 18:189–202

Gao T, Li WZ, Liang SH, Li XH, Ren DM (2007) Enzymatic synthesis of 6-methylpurine-2'-deoxyriboside by recombinant purine nucleoside phosphorylase. Ind Microbiol 37(1):8–13

Hughes BW, Wells AH, Bebok Z (1995) Bystander killing of melanoma cells using the human tyrosinase promoter to express the *Escherichia coli* purine nucleoside phosphorylase gene. Cancer Res 55:3339–3345

Jensen KF, Nygaard P (1975) Purine nucleoside phosphorylase form *Salmonella typhimurium* and *Escherichia coli*. Purification and some properties. Eur J Biochem 51:253–265

Kim BK, Cha S, Parks RE (1968) Purine nucleoside phosphorylase from human erythrocytes: II. Kinetic analysis and substrate-binding studies. J Biol Chem 243:1771–1776

Koszalka GW, Vanhooke J, Steven AS, Hall WW (1988) Purification and properties of inosine-guanosine phosphorylase from *Escherichia coli* K-12. J Bacteriol 170:3493–3498

Krenitzky T, Koszalka G (1981) Purine nucleoside synthesis, an efficient method employing nucleoside phosphorylases. Biochemistry 20:3615–3621

Li XH, Sun JK, Gao T, Ren DM (2006) Cloning and expression of purine nucleoside phosphorylase in *Escherichia coli*. Ind Microbiol 36(3):8–13

Ling F, Inuoe Y, Kimura A (1994) Induction, purification and utilization of purine nucleoside phosphorylase and uridine phosphorylase from *Klebsiella* sp. Process Biochem 29:355–361

Lorentzen MS, Moe E, Jouve HM, Willassen NP (2006) Cold adapted features of *Vibrio salmonicida* catalase: characterization and comparison to the mesophilic counterpart from *Proteus mirabilis*. Extremophiles 10:427–440

Murakami K, Tsushima K (1975) Crystallization and some properties of purine nucleoside phosphorylase from chicken liver. Biochim Biophys Acta 384:390–398

Parks RE, Agarwal RP (1972) Purine nucleoside phosphorylase. Enzymes 7:483–514

Pugmire MJ, Ealick SE (2002) Structural analysis reveals two distinct families of nucleoside phosphorylases. Biochem J 361:1–25

Ropp A,Traut TW (1991) Allosteric regulation of purine nucleoside phosphorylase. Arch Biochem Biophys 288:614–620

Sambrook J, Russell D (2002) Molecular cloning: a laboratory manual. 3rd end. Science Press, Beijing

Sorscher EJ, Peng S, Bebok Z, Allan PW, Bennett LL Jr, Parker WB (1994) Tumour bystander killing in colonic carcinoma utilizing the *Escherichia coli* deoD gene to generate toxic purines. Gene Ther 1:233–238

Stoeckler JD, Agarwal RP, Agarwal KC, Parks RE (1978) Purine nucleoside phosphorylase from human erythrocytes. Methods Enzymol 51:530–538

Tebbe J, Wielgus-Kutrowska B, Schroeder W, Luic M, Shugar D,Saenger W, Koellner G, Bzowska A (1997) Purine nucleoside phosphorylase (PNP) from *Cellulomonas* sp., a different class of PNP different from both "low-molecular weight" mammalian and "high molecular weight" bacterial PNPs. Protein Eng 10(Suppl.):90

Thompson JD, Gibson TJ, Plewniak F, Jeanmougin F, Higgins DG (1997) The CLUSTAL_X windows interface: flexible strategies for multiple sequence alignment aided by quality analysis tools. Nucleic Acids Res 25:4876–4882

Utagawa T, Hirokazu M, Fumihiro Y (1985) Microbiological synthesis of adeninearabinoside. Agric Biol Chem 49(4):1053–1058

Yang Z, Parker WB, Sorscher EJ, Ealick SE (2005) PNP Anticancer gene therapy. Curr Topics Med Chem 5:1259–1274